



Hydrothermal Liquefaction of Scrap Tires: Optimization of Reaction Conditions and Recovery of High Value-Added Products

Rongjie Chen, Hang Li, Kaile Li, Shiyu Zhang, Qinghai Li, Hui Zhou* and Yanguo Zhang*

Key Laboratory for Thermal Science and Power Engineering of Ministry of Education, Beijing Key Laboratory of CO₂ Utilization and Reduction Technology, Department of Energy and Power Engineering, Tsinghua University, Beijing, China

Response surface method (RSM) was proposed to investigate the conversion of scrap tire via hydrothermal treatment. Temperature was the dominant factor in the process. The liquefaction rate increased sharply with temperature and exceeds 40 wt.% in the supercritical region (>374.3°C). A maximum of more than 40 wt.% liquefaction rate was obtained when the tire was kept at 399°C for 60 min with the water/tire mass ratio of 10.8/1. Subsequently, the analysis of solid phase and liquid products at 360 and 400°C was carried out. The thermal stability of natural rubber in tire is significantly deteriorated after hydrothermal treatment. The hydrothermal process of rubber includes chain cleavage, particle hydrolysis, and carbon nanospheres formation, growth and agglomeration. The liquid products including carotenoids, ketones, and aromatic compounds, the ratio of which can be adjusted according to the temperature.

Keywords: hydrothermal liquefaction, scrap tire, response surface methodology, carbon nanospheres, reaction mechanism

OPEN ACCESS

Edited by:

Jalel Labidi,
University of the Basque Country,
Spain

Reviewed by:

Józef Haponiuk,
Gdansk University of Technology,
Poland

Hallil Durak,
Yüzüncü Yıl University, Turkey

*Correspondence:

Hui Zhou
zhouhui.10@tsinghua.org.cn
Yanguo Zhang
zhangyg@tsinghua.edu.cn

Specialty section:

This article was submitted to
Bioenergy and Biofuels,
a section of the journal
Frontiers in Energy Research

Received: 22 December 2021

Accepted: 24 January 2022

Published: 15 February 2022

Citation:

Chen R, Li H, Li K, Zhang S, Li Q,
Zhou H and Zhang Y (2022)
Hydrothermal Liquefaction of Scrap
Tires: Optimization of Reaction
Conditions and Recovery of High
Value-Added Products.
Front. Energy Res. 10:841752.
doi: 10.3389/fenrg.2022.841752

INTRODUCTION

As one of the fastest-growing solid wastes, scrap tires have brought severe challenges to social governance with the increase in automobile production in the past few decades. At the end of 2018, China had produced a total of 816 million rubber tires, of which automobile tires accounted for about 80%, which inevitably caused a sharp increase in the number of discarded tires (Wang et al., 2020). Scrap tires are inherently non-biodegradable, resistant to photochemical decomposition, abrasion, and corrosion (Chen et al., 2019a; Chen et al., 2019b; Okoye et al., 2021). They were generally landfilled or directly burned. Landfill may generate leachate, which can destroy the soil and breed bacteria. During combustion, the high concentrations of N, S, halogen elements, and heavy metals in tires will be released into the atmosphere with high-temperature flue gas, causing serious air pollution (Peng, 2017; Bockstal et al., 2019). To dispose of scrap tires harmlessly, more value-added technologies should be developed (Czajczyńska et al., 2017; Li et al., 2020).

Hydrothermal liquefaction is a promising technology for solid waste treatment. Compared with traditional thermochemical technology (such as combustion, pyrolysis) (Aysu and Durak, 2015; Durak and Aysu, 2015; Yücedağ and Durak, 2019), it has the characteristics of high processing efficiency and low emission. In a closed water-filled environment, organic and inorganic components are degraded at elevated temperatures and pressures, converting the solid waste into liquid products such as acetic acid and crude oil (Baroutian et al., 2013; Déniel et al., 2016; Grigoras et al., 2017; Al-Hammadi et al., 2018; Durak, 2020). Moreover, the “near-zero-emission” of waste treatment can be



FIGURE 1 | Schematic diagram of the tire recycling process and concept through hydrothermal treatment.

realized by subsequently adding oxidants and other methods. Furthermore, the hot pressurized water, at sub- or super-critical region, has some special properties such as low dielectric constant and low density, which make water a non-polar solvent with high solubility and diffusibility and greatly accelerate the reaction rate (Sienkiewicz et al., 2017; Al-Muntaser et al., 2020). On account of the great potential of hydrothermal liquefaction in solid waste treatment, this technology has been applied to convert biomass and other solid waste into energy and resource through harmless treatment (Huang et al., 2019; Beims et al., 2020; Zhan et al., 2020).

Previous studies have demonstrated that temperature and retention time have prominent effects on tire heavy oil yield (Ahmad et al., 2020). For example, Toenh et al. (Park and Gloyna, 1997) found that the oil yield and viscosity peaked at 400°C when the temperature rose from 350 to 450°C. A further study conducted by Zhang et al. (Zhang et al., 2016) indicated that the yield of the liquid products was constant at a temperature of 370–400°C, while the liquid phase product might be degraded into volatile products above 400°C. Unlike the temperature, as the reaction time prolonged, the extent of depolymerization of the tire gradually increased, but it remained constant beyond 100 min due to complete depolymerization of volatiles (Chen et al., 1995). Zhang et al. (2016) also mentioned that the yield of liquid phase product was enhanced as the water/solid mass ratio increased from 0 to 4:1.

Firstly, current research on the hydrothermal liquefaction of tires mainly took the “one factor at a time” (OFAT) method to quantify the impact of a single factor on heavy oil production. However, the interactions between different factors have not been investigated, which cannot be neglected. Secondly, as the main by-product of tire hydrothermal treatment, the research on the properties of liquid products has been blank. Finally, the reaction mechanism of the hydrothermal conversion of tire rubber to carbon remains unclear (Chen et al., 1995; Park and Gloyna, 1997; Zhang et al., 2016; Ahmad et al., 2020).

This work investigates the effect of interactions among temperature, holding time, and water/solid ratio on the hydrothermal liquefaction of scrap tires using the response surface method (RSM) for the first time. The quadratic polynomial fitting was performed to analyze the experimental data and optimize the reaction conditions. Moreover, the main hydrolysis products (solid and liquid phase) of scrap tire were characterized to investigate their possible conversion mechanism in the hydrothermal process. The produced solid and liquid products in this study have the potential to be used as value-added chemicals and/or fuels to realize the waste reduction and resource recycling (Figure 1).

MATERIALS AND METHODS

Materials

The scrap tire (ST) was supplied by Huayi Rubber Co., Ltd. (Sichuan, China). Prior to the experiments, the ST sample was ground and sieved to <250 μm then dried overnight at 105°C. The proximate and ultimate analyses (CHNS) of the feedstock were performed with the thermal differential analyzer (Thermostep) and elemental analyzer (Flash EA3000), respectively. The higher heating value (HHV) was calculated by Dulong formula (Lorry, 1947), i.e., $HHV \text{ (MJ/kg)} = 0.3383C + 1.422(H - O/8)$, as shown in **Supplementary Table S1**. Deionized water (General Reagent), n-hexane (>99.5%, Concord Technology), and acetone (analytical grade, Peking Reagent) were used as received.

Experimental Setup

The laboratory-scale batch reactor (**Supplementary Figure S1**) was custom-made by Songling Chemical Equipment Co., Ltd. (Yantai, Shandong, China). The reactor vessel was made of S30408 stainless steel with an effective volume of 100 ml (I.D.

25, O.D. 55 mm, inner height 21 cm). The maximum operating temperature and pressure of the setup are 400°C and 30 MPa, respectively. The reactor was heated by a 2 kW electric furnace, and the temperature accuracy was within $\pm 0.5^\circ\text{C}$.

In a typical experiment, 60 g of deionized water and 5.0–7.5 g of tire sample (water/tire ratio 8–12) were loaded into the reactor. The reactor was then sealed and purged with high-purity nitrogen (>99.999%) three times to remove residual air to ensure an inert atmosphere inside. The initial pressure of the experiment is atmospheric. After that, the reactor was heated to the set temperature (360–400°C) under stirring (300 rpm), kept for a designed retention time (20–60 min), and then cooled to <50°C with a high-speed fan. Duplicate experiments were carried out, and the discrepancy was 5.4%, which is acceptable in current work.

Separation of the Reaction Products

The yield of gas in this study was negligible, and thus it has not been specifically collected. The solid/liquid mixture in the reactor was filtered through a pre-weighed Whatman No. 5 filter paper (2.5 μm pore size, dried before use) under reduced pressure. The filtrate was collected and extracted with n-hexane (filtrate: n-hexane = 2:1) for subsequent GC-MS analysis of the liquid products. Afterward, the inner wall, top cover, and stirring blade of the reactor were rinsed with acetone several times to ensure that the adhering solids and heavy oil were completely collected. The mixture containing the solid product and the acetone phase was thoroughly stirred and vacuum filtered and washed with acetone until the filtrate became colorless. The obtained solid product was dried overnight at 105°C and then weighed to determine the yield of the solid residue (SR). The liquefaction rate (LR) of scrap tire was calculated from Eq. 1:

$$\text{LR} = \left(1 - \frac{\text{mass of SR}}{\text{mass of tire}} \right) * 100\% \quad (1)$$

Characterization

The thermogravimetric (TG) analysis was conducted in a NETZSCH STA 409C/3/F instrument under a nitrogen atmosphere. About 10 mg of sample was uniformly placed into a crucible and heated to 800°C at a heating rate of 20°C min⁻¹. Scanning electron microscopy (SEM) of the solid materials was performed on Zeiss Field Emission Scanning Electron Microscope (Merlin, Zeiss, Germany).

The liquid products were extracted by hexane and then analyzed by a gas chromatography-mass spectrometry [GC (Trace 1,300), MS (ISQ OD), Thermo Scientific, United States] equipped with a TG-5SILMS column (30 m \times 0.25 mm ID \times 0.25 μm , cross chromatography). High-purity helium (>99.9%) was used as the carrier gas. The oven temperature program was: keeping as 35°C for 1 min, ramping up 200°C at 5°C min⁻¹, and then heating to 250°C at 10°C min⁻¹.

Design of Experiments

Box-Behnken Design (BBD) is one of the most widely used RSM designs due to its advantages in using experimental data to construct analysis models (Cobas et al., 2014; Yadav et al.,

2021). Therefore, we used BBD to investigate the influence of different experimental conditions on the liquefaction rate and optimize the conditions through modeling. As listed in **Supplementary Table S2**, based on previous work (Zhang et al., 2016; Chen et al., 2019a) and some preliminary experiments, three variables, i.e., temperature (360–400°C), reaction time (20–60 min), and water/tire ratio (8:1–12:1) were investigated. The boundary and intermediate values of each variable were selected as experimental conditions. The design contained a total of 17 experiments (12 factorial points and 5 center points), as shown in **Table 1** (*vide infra*). The data matrix was analyzed by Design Expert 8.0.4 to quantify the comprehensive influence of these factors and determine the optimal combination. To obtain the linear, quadratic, and interaction effects of the three variables on the results, regression analysis was applied, and the established quadratic polynomial model can be expressed as Eq. 2:

$$Y = \alpha_0 + \sum_{i=1}^3 \alpha_i X_i + \sum_{i=1}^3 \alpha_{ii} X_i^2 + \sum_{i=1}^3 \sum_{j>1}^3 \alpha_{ij} X_i X_j \quad (2)$$

where Y denotes the output response (liquefaction rate), X_i and X_j represent the experimental variables, α_0 represents the constant term of the model, α_{ii} , α_{ij} , and α_{ij} are the linear term coefficient, quadratic term coefficient and interaction coefficient of the model, respectively. After the establishment of the model, analysis of variance was performed on the regression model to test the quality of model fitting, and p -test and F -test were used to verify the statistical significance of the model.

RESULTS AND DISCUSSION

RSM Results and Response Surface

Analysis

Model Fitting

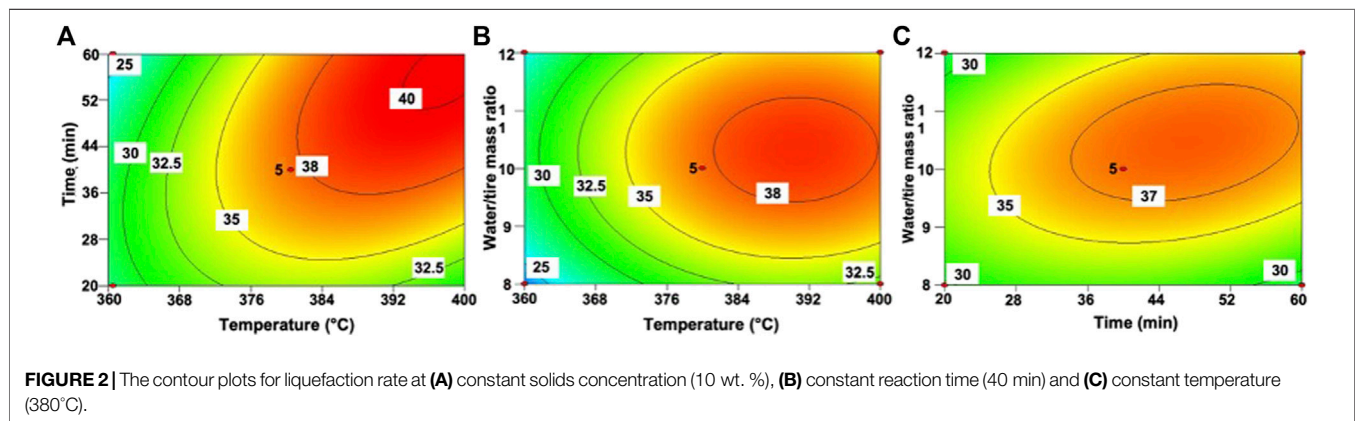
The liquefaction rate of the tire under different reaction conditions is exhibited in **Table 1**, which varies between 20.7 wt.% and 39.7 wt.%. The values were much higher than the conversion rate of pyrolysis at the same temperature (Chen et al., 2019a). Hydrogen and hydroxyl radicals in hot-pressed water attack the polymer backbone, leading to more prone chain scission reactions, proving that hydrothermal treatment has significant advantages in waste tire disposal. Based on these data, the fitting quadratic equation of the liquefaction rate is displayed in Eq. 3.

$$Y = 37.63 + 4.45X_1 + 1.44X_2 + 1.33X_3 + 3.67X_1X_2 + 0.22X_1X_3 + 2.02X_2X_3 - 4.28X_1^2 - 2.78X_2^2 - 4.44X_3^2 \quad (3)$$

The analysis of variance (ANOVA) was performed on the regression model (**Supplementary Table S3**). The model was found to be significant, with a p -value of 0.0064, much lower than 0.05. In addition, the p -value of lack of fit was 0.0659 (larger than 0.05), indicating that the lack of fit is not significant, which signified that the model fits well.

TABLE 1 | The liquefaction rate of tire under different conditions (BBD).

	Temperature (X_1)	Time (X_2)	Water/tire mass ratio (X_3)	Liquefaction rate (Y , wt.%)
1	360	20	10:1	30.8
2	400	20	10:1	28.3
3	360	60	10:1	25.5
4	400	60	10:1	37.7
5	360	40	8:1	20.7
6	400	40	8:1	33.2
7	360	40	12:1	24.2
8	400	40	12:1	37.6
9	380	20	8:1	29.9
10	380	60	8:1	29.6
11	380	20	12:1	27.2
12	380	60	12:1	35.0
13	380	40	10:1	35.5
14	380	40	10:1	37.3
15	380	40	10:1	39.7
16	380	40	10:1	37.5
17	380	40	10:1	38.2



To study the applicability of the model, the normal probability and residual plots of the liquefaction rate were established, as displayed in **Supplementary Figure S2**. Typically, each point on a normal probability plot should be located approximately on a straight line, from which it can be inferred that the prediction is real. As can be seen from **Supplementary Figure S2A**, the plotted data roughly formed a straight line, which showed the normal distribution of the residual fitting of the liquefaction and proved that the model demonstrated good agreement with the experimental data. Besides, the residual plot in **Supplementary Figure S2B** showed that the residual liquefaction rate was randomly dispersed and no outliers were observed, which also indicated the accuracy of the model.

Response Surface Plots and Reaction Condition Optimization

According to the determined regression model, the three-dimensional response surface and contour plots of the liquefaction rate based on the temperature, reaction time, and water/tire ratio are shown in **Figure 2**. Based on the contour plots,

we can see strong interactions between variables: the influence of one of them largely depends on the level of the other two variables.

The effects of temperature and reaction time on the liquefaction rate are shown in **Figure 2A**, which indicates that in the selected experimental conditions, the liquefaction rate increased monotonously with increasing temperature and time. The liquefaction rate was more sensitive to temperature than reaction time, which was consistent with the conclusions in the literature (Jindal and Jha, 2016; Zhang et al., 2016; Chan et al., 2018). It can be observed that as the temperature rose from 362 to 392°C, the liquefaction rate increased sharply and exceeded 40% in a certain interval. Moreover, at low temperatures (<368°C), increasing the reaction time (from 20 to 60 min) did not improve the liquefaction rate. The reason is that the main components of tires (natural rubber and styrene-butadiene rubber) have very high bond energy for molecular chain cleavage, which is difficult to break at low temperatures. When the temperature is higher than 380°C, prolonging the reaction time significantly promotes the depolymerization of the tire into small molecules in supercritical water.

TABLE 2 | Optimum operating conditions and liquefaction rate.

Optimum conditions			Maximum liquefaction rate (wt.%)		
Temperature (C)	Reaction time (min)	Water/tire ratio	Predicted	Experimental	Discrepancy
399.2	60	10.8	40.9	38.8	5.4

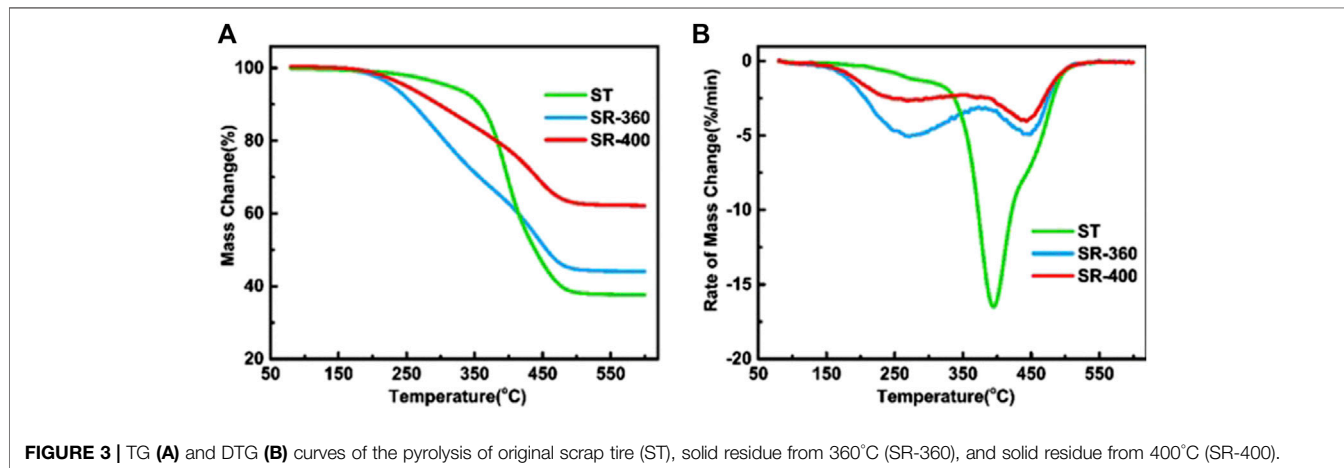
**FIGURE 3** | TG (A) and DTG (B) curves of the pyrolysis of original scrap tire (ST), solid residue from 360°C (SR-360), and solid residue from 400°C (SR-400).

Figure 2B illustrates the effect of reaction temperature and water/tire ratio on the liquefaction rate. Compared with the water/tire ratio, the temperature played a more significant role in the liquefaction of waste tire. Especially in the supercritical region ($>374.3^{\circ}\text{C}$), the rapid changes in the dielectric constant and density of water lead to its high diffusibility and organic solubility, and thus the efficiencies of hydrothermal reactions were greatly enhanced (Kruse and Dinjus, 2007; Wen et al., 2009). On the whole, the increase in temperature showed a tendency to increase the liquefaction rate. In the hydrothermal process, the water acted as both a solvent and a reactant to participate in the depolymerization reaction of tire (Zhang et al., 2016). Unlike the monotonous effect of temperature, there is an optimal water/tire ratio during the thermal liquefaction of tires. Keeping the temperature constant, the liquefaction rate increased first and then decreased with the increase of the water/tire ratio, with the optimal water/tire ratio of ca. 10. A low water/tire ratio cannot provide sufficient solubility for small molecule products or intermediates, thereby slowing down the rate of depolymerization of solid materials. Excessive water was also not conducive to the liquefaction of raw materials and caused a decrease in volumetric efficiency and productivity, and an increase in downstream wastewater treatment costs. The liquefaction rate reached the maximum value of ca. 40% when the temperature was 384–394°C and the water/tire ratio was 9.5–11.0 as shown in **Figure 2B**.

The effect of reaction time and water/tire ratio on liquefaction rate is shown in **Figure 2C**. The influence of reaction time was closely related to the water/tire ratio. As the water/tire ratio increased, the influence of reaction time on the liquefaction rate became stronger. For example, when the water/tire ratio was 8 and the reaction time was extended from 20 to 40 min, the

liquefaction rate only increased by approximately 2%. When the water/tire ratio was 12, this value was improved by nearly 6%. Similarly, when the holding time was longer, the influence of the water/tire ratio on the liquefaction rate was intensified.

Table 2 lists the optimal values of the process variables at the maximum liquefaction rate. In order to verify the predicted optimization results, two sets of confirmatory experiments were carried out under the optimal predicted conditions, i.e., $T = 399.2^{\circ}\text{C}$, $t = 60$ min, water/tire ratio = 10.8. The results show that the experimental value was in good agreement with the model predicted value, and the discrepancy was as low as 5.4%. Therefore, RSM can be used as an effective tool for optimizing the operating conditions of the hydrothermal liquefaction of waste tires.

Product Analysis

As mentioned earlier, the gas yields were neglectable. Considering that temperature is the dominant variable in the hydrothermal conversion of tires, this study focused on the properties of solid and water phase products at different temperatures (360 and 400°C, reaction time and water-to-tire mass ratio were 40 min and 10:1, respectively).

Analysis of Solid Residue

TG analysis was carried out to examine the thermal stability of the ST and solid residue from hydrothermal reactions. As shown in **Figure 3**, the pyrolysis of ST started at ca. 200°C and ended at ca. 500°C. A main peak was observed at approximately 395°C in the DTG curve, which demonstrated the existence of a considerable amount of natural rubber (NR) in ST (Singh et al., 2018). The shoulder peak near 450°C was attributed to the decomposition of synthetic rubber (Wang et al., 2019). Compared with the raw

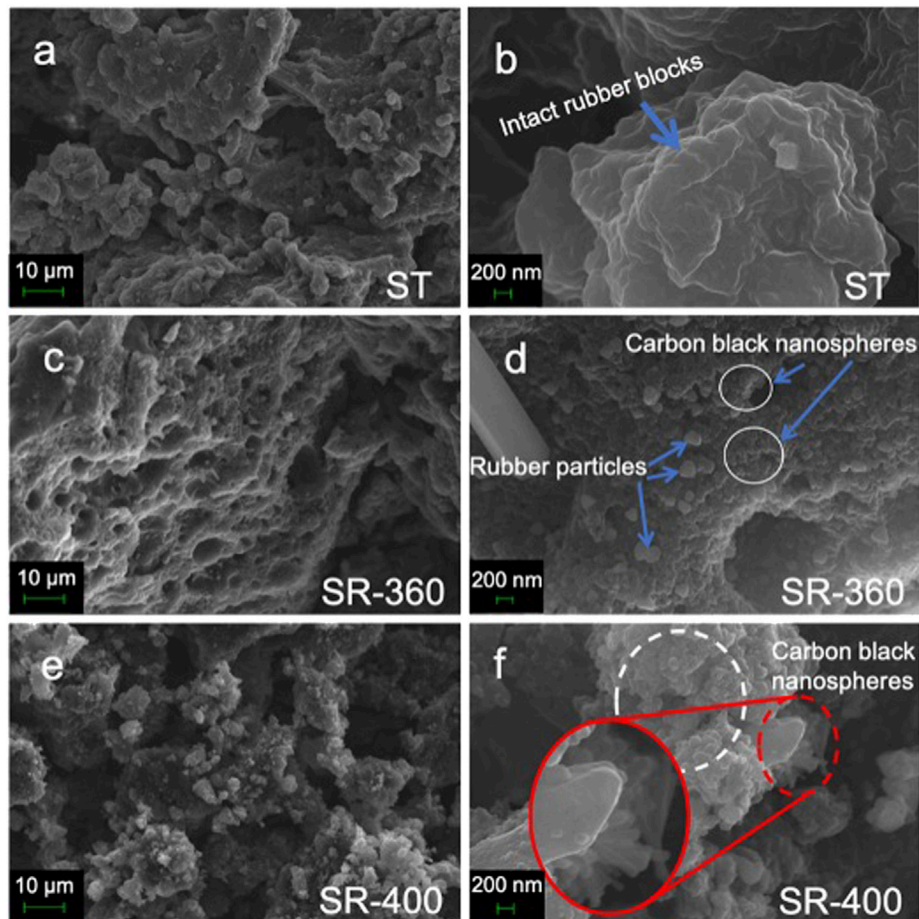


FIGURE 4 | SEM of tire powder and solid residue from hydrothermal treatment. **(A, B)** original scrap tire (ST). **(C, D)** solid residue from 360°C (SR-360). **(E, F)** solid residue from 400°C (SR-400).

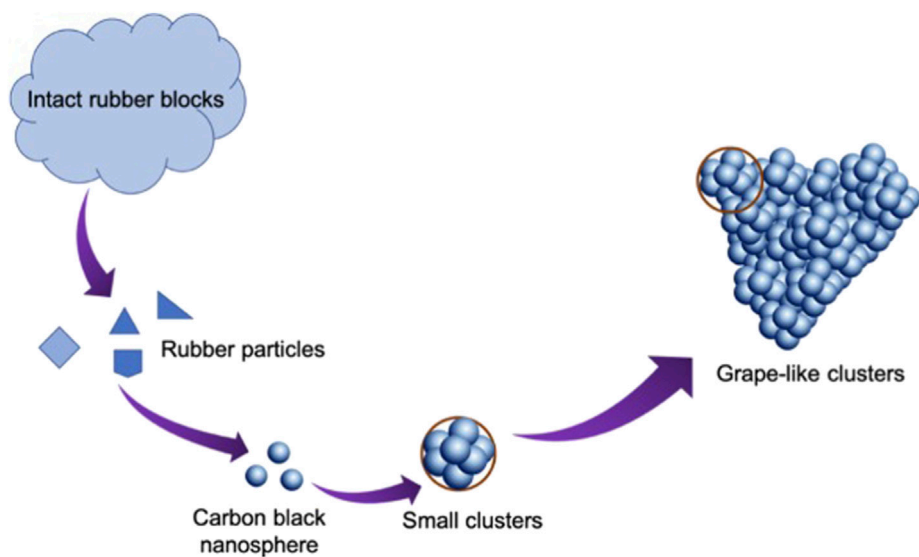
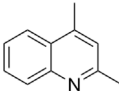
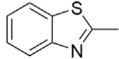

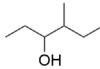
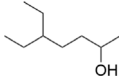
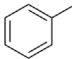
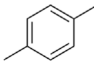
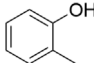
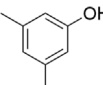
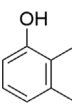
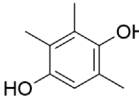
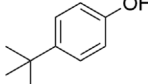
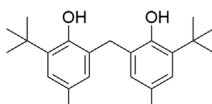
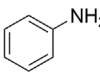
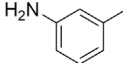


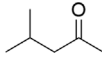
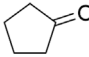
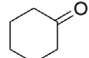
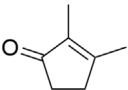
FIGURE 5 | The mechanism of the formation of carbon black clusters during the hydrothermal treatment of tire rubber.

TABLE 3 | Major organic compounds in the liquid phase at different reaction conditions.

Compounds	Structure	Rt/min	Peak area/ $\times 10^6$ (360 °C)	Peak area/ $\times 10^6$ (400 °C)
Tire additive derivatives 2,4-Dimethyl-quinoline		13.2	3.7	2.8
2-Methyl-benzothiazole		10.8	2.2	2.3
Carotenoids Carotenoids		25.1	33.0	25.3
Alcohols 4-Methyl-3-hexanol		3.1	/	0.7
5-Ethyl-2-heptanol		4.4	/	0.8
Benzene derivatives Toluene		3.4	1.4	1.8
p-Xylene		4.8	1.4	/
Phenolic compounds 2-Methyl-phenol		7.5	/	2.0
3,5-Dimethyl-phenol		9.0	/	0.9
2,3-Dimethyl-phenol		9.0	1.1	0.7
2,3,5-Trimethyl-1,4-benzenediol		10.1	/	1.3
P-tert-butyl-Phenol		11.5	2.5	3.2
Phenol-2,2'-Methylenebis [6-(1,1-dimethylethyl)-4-methyl		22.9	1.0	/
Anilines Aniline		6.4	9.1	17.2
3-Methyl-benzenamine		7.9	0.9	/

(Continued on following page)

TABLE 3 | (Continued) Major organic compounds in the liquid phase at different reaction conditions.

Compounds	Structure	Rt/min	Peak area/ $\times 10^6$ (360 °C)	Peak area/ $\times 10^6$ (400 °C)
Ketones				
Methyl isobutyl ketone		3.1	10.8	8.9
Cyclopentanone		3.7	1.6	2.2
Cyclohexanone		5.1	7.0	7.0
2,3-Dimethyl-1-one-2-cyclopenten		7.3	/	0.8

material, the solid residue after hydrothermal treatment performed distinct degradation characteristics. As shown in **Figure 3A**, the residue yields of ST, SR-360, and SR-400 after pyrolysis at 600°C in TGA were 38 wt.%, 44 wt.%, and 62 wt.%, respectively. The residue amount of SR-360 after pyrolysis was very close to that of the ST sample, which means that even after 60 min of hydrothermal treatment at 360°C, most of the volatile matter in the feedstock remains unconverted. Nevertheless, it is worth noting that hydrothermal treatment significantly reduces the thermal stability of NR in tires. As shown in **Figure 3B**, the weight loss peak caused by the decomposition of NR has moved from 400 to 270°C. This indicates that the cross-linked structure of NR molecules may undergo rearrangement and isomerization reactions, finally forming a thermally unstable structure in hot-pressed water. Therefore, hydrothermal pretreatment can be a promising method in the thermochemical utilization of scrap tires under mild conditions.

Figure 4 displays the overall morphology of different solid samples. It can be observed that the original rubber were bulks with no pores (**Figure 4A**). After the hydrothermal treatment, part of the rubber dissolved from the surface and then hydrolyzed, forming a loose and porous void structure on the surface, while the majority of the rubber remained unconverted at 360°C, as shown in **Figure 4C**. As the temperature further increased to 400°C, the hydrolysis reaction intensified. **Figure 4E** indicated that a high proportion of grains were produced, and lumpy rubber particles almost disappeared. At 400°C, the tire rubber was more severely degraded compared with 360°C. High-resolution SEM showed that the ST sample was a rubber particle with an intact and dense surface (**Figure 4B**). In the hot-pressed water at 360°C, the rubber fibers were broken into small particles, some of which further participated in the hydrolysis reaction to form agglomerates of carbon black nanospheres (ca. 40 nm) (Li et al., 2005; Al-Hammadi et al., 2018) (**Figure 4D**). After further hydrothermal treatment at 400°C, a large number of carbon black spheres agglomerated into graph-like clusters with irregular appearances. There were still some lumps or rods of rubber particles with inconsistent sizes (**Figure 4F**), indicating that the tire rubber has not been completely converted at 400°C.

To summarize, the macromolecular rubber fiber first decomposes into massive particles in the hydrothermal environment at elevated temperatures (**Figure 5**). Some of these particles participate in further hydrolysis to form carbon black nanospheres. Subsequently, some carbon black spheres are encased by other spheres to form a small cluster. Furthermore, the agglomeration of small clusters forms a grape-like structure.

Analysis of the Liquid Products

To investigate the liquid products, we performed the GC-MS analysis, where carotenoids, aromatic compounds, ketones, and alcohols were detected (**Table 3**). Carotenoids, chain or cyclic ketones, and alcohols were generated from polyisoprene in natural rubber (Ahmad et al., 2019; Li et al., 2020), while aromatic compounds were derived from styrene-butadiene rubber (Kar, 2011). Besides, nitrogen and sulfur compounds are mainly converted from tire additives (Laresgoiti et al., 2004; Zhang et al., 2016).

In the hydrothermal environment, the macromolecular long-chain polyisoprene depolymerized into a helical structure of chain-like hydrocarbons with a carotenoid main structure under the attack of water molecules. It has chemically active methoxy groups at both ends, which can be used as precursors for carotenoid synthesis. As the temperature increased from 360 to 400°C, the deepening of the hydrolysis of natural rubber did not lead to an increase in its content, but a 23% decrease. Carotenoids are relatively weak in thermal stability at high temperatures and will be broken down into smaller molecular hydrocarbons or oxygen-containing compounds. This can also be demonstrated by the short-chain alcohol compounds that appear at 400°C. Similarly, the proportion of methyl isobutyl ketone had a decrease (18%) at elevated temperatures. Cyclic ketones were reported to be unstable in a hydrothermal environment, but the content of cyclic ketones remained fairly static at different temperatures. It can be inferred that its decomposition and generation have reached a dynamic balance.

Moreover, as the temperature increased to 400°C, the content of anilines and phenols increased significantly due to the decomposition of styrene-butadiene rubber (Cunliffe and Williams, 1998; Mastral et al., 2000). The styrene-butadiene

rubber was first depolymerized into styrene monomer, and then the connection between the vinyl group and the benzene ring was impacted by the amine group from the additives (such as benzothiazoles, thioureas, thiuram, amines, etc.) (Laresgoiti et al., 2004) and water molecules to form anilines and phenols in the supercritical water (400°C). The original rubber vulcanization accelerators may also decompose into anilines in the hydrothermal process.

Our results showed that the liquid phase from tire hydrothermal treatment contained diverse valuable chemicals with considerably high content, which were key precursors and intermediates in the chemical industry. In addition, the desired chemicals can be selectively obtained by adjusting the reaction temperature. For example, an increase in temperature was conducive to the formation of aromatic compounds, but it also caused a large amount of cracking of carotenoids' molecular chain.

CONCLUSION

The conversion of scrap tire to valuable products *via* hydrothermal treatment was studied. The model established by RSM fitted the experimental data well and revealed the influence of the interactions between variables (temperature, reaction time, and water/tire ratio) on the liquefaction rate. Temperature was the dominant factor. Reaction time has little effect at low temperatures (<368°C). Water/tire ratio was a key parameter in the hydrothermal process, due to that insufficient or excessive water would reduce the liquefaction rate. A maximum of 40.9 wt.% liquefaction rate was obtained when tire was kept at 399°C for 60 min with the water/solid mass ratio of 10.8. The cross-linked structure of NR molecules may undergo rearrangement and isomerization reactions, forming a thermally unstable structure in hot-pressed water. Scanning electron microscopy revealed that the hydrothermal mechanism of tires includes structure cleavage, particle hydrolysis, and carbon nanosphere formation, growth and agglomeration. Our results proved that the liquid products of

tire hydrothermal treatment contained diverse valuable chemicals with considerably high content, such as carotenoids, ketones, and aromatic compounds, which were key precursors and intermediates in the chemical industry. Moreover, the proportion of some chemicals could be adjusted to some extent by changing the process parameters.

DATA AVAILABILITY STATEMENT

The original contributions presented in the study are included in the article/**Supplementary Material**, further inquiries can be directed to the corresponding authors.

AUTHOR CONTRIBUTIONS

RC: Conceptualization, Methodology, Software, Writing (original draft). HL: Investigation, Experiment, Writing (original draft). KL: Kinetic calculation, Validation. SZ: Writing (revised draft). QL: Project administration, Supervision. HZ: Methodology, Conceptualization, Writing—review and; editing. YZ: Conceptualization, Supervision, Writing—review and; editing.

FUNDING

This work was supported by the National Natural Science Foundation of China (grant number 52070116) and the Tsinghua University-Shanxi Clean Energy Research Institute Innovation Project Seed Fund.

SUPPLEMENTARY MATERIAL

The Supplementary Material for this article can be found online at: <https://www.frontiersin.org/articles/10.3389/fenrg.2022.841752/full#supplementary-material>

REFERENCES

- Ahmad, N., Abnisa, F., and Daud, W. M. A. W. (2019). Synthesis of Liquid Fuel through Hydrothermal Conversion of Natural Rubber. *AIP Conf. Proc.* 2168 (1), 020058. doi:10.1063/1.5132485
- Ahmad, N., Ahmad, N., Maafa, I. M., Ahmed, U., Akhter, P., Shehzad, N., et al. (2020). Conversion of Poly-Isoprene Based Rubber to Value-Added Chemicals and Liquid Fuel via Ethanolysis: Effect of Operating Parameters on Product Quality and Quantity. *Energy* 191, 116543. doi:10.1016/j.energy.2019.116543
- Al-Hammadi, S. A., Al-Absi, A. A., Bin-Dahman, O. A., and Saleh, T. A. (2018). Poly(trimesoyl Chloride-Melamine) Grafted on Palygorskite for Simultaneous Ultra-trace Removal of Methylene Blue and Toxic Metals. *J. Environ. Manage.* 226, 358–364. doi:10.1016/j.jenvman.2018.08.025
- Al-Muntaser, A. A., Varfolomeev, M. A., Suwaid, M. A., Yuan, C., Chemodanov, A. E., Feoktistov, D. A., et al. (2020). Hydrothermal Upgrading of Heavy Oil in the Presence of Water at Sub-critical, Near-Critical and Supercritical Conditions. *J. Pet. Sci. Eng.* 184, 106592. doi:10.1016/j.petrol.2019.106592
- Aysu, T., and Durak, H. (2015). Catalytic Pyrolysis of Liquorice (Glycyrrhiza Glabra L.) in a Fixed-Bed Reactor: Effects of Pyrolysis Parameters on Product Yields and Character. *J. Anal. Appl. Pyrolysis* 111, 156–172. doi:10.1016/j.jaap.2014.11.017
- Baroutian, S., Robinson, M., Smit, A.-M., Wijeyekoon, S., and Gapes, D. (2013). Transformation and Removal of wood Extractives from Pulp Mill Sludge Using Wet Oxidation and thermal Hydrolysis. *Bioresour. Tech.* 146, 294–300. doi:10.1016/j.biortech.2013.07.098
- Beims, R. F., Hu, Y., Shui, H., and Xu, C. (2020). Hydrothermal Liquefaction of Biomass to Fuels and Value-Added Chemicals: Products Applications and Challenges to Develop Large-Scale Operations. *Biomass and Bioenergy* 135, 105510. doi:10.1016/j.biombioe.2020.105510
- Bockstal, L., Berchem, T., Schmetz, Q., and Richel, A. (2019). Devulcanisation and Reclaiming of Tires and Rubber by Physical and Chemical Processes: A Review. *J. Clean. Prod.* 236, 117574. doi:10.1016/j.jclepro.2019.07.049
- Chan, Y. H., Quitain, A. T., Yusup, S., Uemura, Y., Sasaki, M., and Kida, T. (2018). Optimization of Hydrothermal Liquefaction of palm Kernel Shell and Consideration of Supercritical Carbon Dioxide Mediation Effect. *J. Supercrit. Fluids* 133, 640–646. doi:10.1016/j.supflu.2017.06.007
- Chen, D. T., Perman, C. A., Riechert, M. E., and Hoven, J. (1995). Depolymerization of Tire and Natural Rubber Using Supercritical Fluids. *J. Hazard. Mater.* 44 (1), 53–60. doi:10.1016/0304-3894(95)00047-x

- Chen, R., Lun, L., Cong, K., Li, Q., and Zhang, Y. (2019a). Insights into Pyrolysis and Co-pyrolysis of Tobacco Stalk and Scrap Tire: Thermochemical Behaviors, Kinetics, and Evolved Gas Analysis. *Energy* 183, 25–34. doi:10.1016/j.energy.2019.06.127
- Chen, R., Zhang, J., Lun, L., Li, Q., and Zhang, Y. (2019b). Comparative Study on Synergistic Effects in Co-pyrolysis of Tobacco Stalk with Polymer Wastes: Thermal Behavior, Gas Formation, and Kinetics. *Bioresour. Tech.* 292, 121970. doi:10.1016/j.biortech.2019.12.1970
- Cobas, M., Sanromán, M. A., and Pazos, M. (2014). Box-Behnken Methodology for Cr (VI) and Leather Dyes Removal by an Eco-Friendly Biosorbent: *F. Vesiculosus*. *Bioresour. Tech.* 160, 166–174. doi:10.1016/j.biortech.2013.12.125
- Cunliffe, A. M., and Williams, P. T. (1998). Composition of Oils Derived from the Batch Pyrolysis of Tyres. *J. Anal. Appl. Pyrolysis* 44 (2), 131–152. doi:10.1016/s0165-2370(97)00085-5
- Czajczyńska, D., Krzyżyńska, R., Jouhara, H., and Spencer, N. (2017). Use of Pyrolytic Gas from Waste Tire as a Fuel: A Review. *Energy* 134, 1121–1131. doi:10.1016/j.energy.2017.05.042
- Déniel, M., Haarlemmer, G., Roubaud, A., Weiss-Hortala, E., and Fages, J. (2016). Optimisation of Bio-Oil Production by Hydrothermal Liquefaction of Agro-Industrial Residues: Blackcurrant Pomace (*Ribes Nigrum* L.) as an Example. *Biomass and Bioenergy* 95, 273–285. doi:10.1016/j.biombioe.2016.10.012
- Durak, H., and Aysu, T. (2015). Effect of Pyrolysis Temperature and Catalyst on Production of Bio-Oil and Bio-Char from Avocado Seeds. *Res. Chem. Intermed* 41 (11), 8067–8097. doi:10.1007/s11164-014-1878-0
- Durak, H. (2020). Hydrothermal Liquefaction of Glycyrrhiza Glabra L. (Liquorice): Effects of Catalyst on Variety Compounds and Chromatographic Characterization. *Energy Sourc. A: Recovery, Utilization, Environ. Effects* 42 (20), 2471–2484. doi:10.1080/15567036.2019.1607947
- Grigoras, I. F., Stroe, R. E., Sintamarean, I. M., and Rosendahl, L. A. (2017). Effect of Biomass Pretreatment on the Product Distribution and Composition Resulting from the Hydrothermal Liquefaction of Short Rotation Coppice Willow. *Bioresour. Tech.* 231, 116–123. doi:10.1016/j.biortech.2017.01.056
- Huang, H.-j., Chang, Y.-c., Lai, F.-y., Zhou, C.-f., Pan, Z.-q., Xiao, X.-f., et al. (2019). Co-liquefaction of Sewage Sludge and rice Straw/wood Sawdust: The Effect of Process Parameters on the Yields/properties of Bio-Oil and Biochar Products. *Energy* 173, 140–150. doi:10.1016/j.energy.2019.02.071
- Jindal, M. K., and Jha, M. K. (2016). Effect of Process Parameters on Hydrothermal Liquefaction of Waste Furniture Sawdust for Bio-Oil Production. *RSC Adv.* 6 (48), 41772–41780. doi:10.1039/c6ra02868c
- Kar, Y. (2011). Catalytic Pyrolysis of Car Tire Waste Using Expanded Perlite. *Waste Manage.* 31 (8), 1772–1782. doi:10.1016/j.wasman.2011.04.005
- Kruse, A., and Dinjus, E. (2007). Hot Compressed Water as Reaction Medium and Reactant: Properties and Synthesis Reactions. *J. Supercrit. Fluids* 39 (3), 362–380. doi:10.1016/j.supflu.2006.03.016
- Laresgoiti, M. F., Caballero, B. M., de Marco, I., Torres, A., Cabrero, M. A., and Chomón, M. J. (2004). Characterization of the Liquid Products Obtained in Tyre Pyrolysis. *J. Anal. Appl. Pyrolysis* 71 (2), 917–934. doi:10.1016/j.jaap.2003.12.003
- Li, D., Lei, S., Lin, F., Zhong, L., Ma, W., and Chen, G. (2020). Study of Scrap Tires Pyrolysis - Products Distribution and Mechanism. *Energy* 213, 119038. doi:10.1016/j.energy.2020.119038
- Li, S.-Q., Yao, Q., Wen, S.-E., Chi, Y., and Yan, J.-H. (2005). Properties of Pyrolytic Chars and Activated Carbons Derived from Pilot-Scale Pyrolysis of Used Tires. *J. Air Waste Manage. Assoc.* 55 (9), 1315–1326. doi:10.1080/10473289.2005.10464728
- Lorry, H. H. (1947). *Chemistry of Coal Utilization*, I. New York: John Wiley & Sons, 138–141.
- Mastral, A. M., Murillo, R., Callen, M. S., and Garcia, T. (2000). Optimisation of Scrap Automotive Tyres Recycling into Valuable Liquid Fuels. *Resour. Conservation Recycling* 29 (4), 263–272. doi:10.1016/s0921-3449(00)00051-3
- Okoye, C. O., Jones, I., Zhu, M., Zhang, Z., and Zhang, D. (2021). Manufacturing of Carbon Black from Spent Tyre Pyrolysis Oil - A Literature Review. *J. Clean. Prod.* 279, 123336. doi:10.1016/j.jclepro.2020.123336
- Park, S., and Gloyna, E. F. (1997). Statistical Study of the Liquefaction of Used Rubber Tyre in Supercritical Water. *Fuel* 76 (11), 999–1003. doi:10.1016/s0016-2361(97)00088-4
- Peng, Y. (2017). Perspectives on Technology for Landfill Leachate Treatment. *Arabian J. Chem.* 10, S2567–S2574. doi:10.1016/j.arabj.2013.09.031
- Sienkiewicz, M., Janik, H., Borzędowska-Labuda, K., and Kucińska-Lipka, J. (2017). Environmentally Friendly Polymer-Rubber Composites Obtained from Waste Tyres: A Review. *J. Clean. Prod.* 147, 560–571. doi:10.1016/j.jclepro.2017.01.121
- Singh, R. K., Ruj, B., Jana, A., Mondal, S., Jana, B., Kumar Sadhukhan, A., et al. (2018). Pyrolysis of Three Different Categories of Automotive Tyre Wastes: Product Yield Analysis and Characterization. *J. Anal. Appl. Pyrolysis* 135, 379–389. doi:10.1016/j.jaap.2018.08.011
- Wang, M., Zhang, L., Li, A., Irfan, M., Du, Y., and Di, W. (2019). Comparative Pyrolysis Behaviors of Tire Tread and Side wall from Waste Tire and Characterization of the Resulting Chars. *J. Environ. Manage.* 232, 364–371. doi:10.1016/j.jenvman.2018.10.091
- Wang, Q.-Z., Wang, N.-N., Tseng, M.-L., Huang, Y.-M., and Li, N.-L. (2020). Waste Tire Recycling Assessment: Road Application Potential and Carbon Emissions Reduction Analysis of Crumb Rubber Modified Asphalt in China. *J. Clean. Prod.* 249, 119411. doi:10.1016/j.jclepro.2019.119411
- Wen, D., Jiang, H., and Zhang, K. (2009). Supercritical Fluids Technology for Clean Biofuel Production. *Prog. Nat. Sci.* 19 (3), 273–284. doi:10.1016/j.pnsc.2008.09.001
- Yadav, A., Yadav, P., Kumar Singh, A., Kumar, V., Chintaman Sonawane, V., MarkandeyaNaresh Bharagava, R., et al. (2021). Decolourisation of Textile Dye by Laccase: Process Evaluation and Assessment of its Degradation Bioproducts. *Bioresour. Tech.* 340, 125591. doi:10.1016/j.biortech.2021.125591
- Yücedağ, E., and Durak, H. (2019). Bio-oil and Bio-Char from *Lactuca Scariola*: Significance of Catalyst and Temperature for Assessing Yield and Quality of Pyrolysis. *Energy Sourc. Part A: Recovery, Utilization, Environ. Effects*, 1–14. doi:10.1080/15567036.2019.1645765
- Zhan, L., Jiang, L., Zhang, Y., Gao, B., and Xu, Z. (2020). Reduction, Detoxification and Recycling of Solid Waste by Hydrothermal Technology: A Review. *Chem. Eng. J.* 390, 124651. doi:10.1016/j.cej.2020.124651
- Zhang, L., Zhou, B., Duan, P., Wang, F., and Xu, Y. (2016). Hydrothermal Conversion of Scrap Tire to Liquid Fuel. *Chem. Eng. J.* 285, 157–163. doi:10.1016/j.cej.2015.10.001

Conflict of Interest: The authors declare that the research was conducted in the absence of any commercial or financial relationships that could be construed as a potential conflict of interest.

Publisher's Note: All claims expressed in this article are solely those of the authors and do not necessarily represent those of their affiliated organizations, or those of the publisher, the editors and the reviewers. Any product that may be evaluated in this article, or claim that may be made by its manufacturer, is not guaranteed or endorsed by the publisher.

Copyright © 2022 Chen, Li, Li, Zhang, Li, Zhou and Zhang. This is an open-access article distributed under the terms of the Creative Commons Attribution License (CC BY). The use, distribution or reproduction in other forums is permitted, provided the original author(s) and the copyright owner(s) are credited and that the original publication in this journal is cited, in accordance with accepted academic practice. No use, distribution or reproduction is permitted which does not comply with these terms.